Chinese Chemical Letters 36 (2025) 109773

Contents lists available at ScienceDirect

Chinese Chemical Letters

journal homepage: www.elsevier.com/locate/cclet

Attenuating reductive decomposition of fluorinated electrolytes for high-voltage lithium metal batteries

Zhen-Zhen Dong[a], Jin-Hao Zhang[a], Lin Zhu[b], Xiao-Zhong Fan[a], Zhen-Guo Liu[a,c,d,*], Yi-Bo Yan[a,*], Long Kong[a,*]

[a] Frontiers Science Center for Flexible Electronics and Xi'an Institute of Flexible Electronics (IFE), Northwestern Polytechnical University, Xi'an 710129, China
[b] Air and Missile Defense College, Air Force Engineering University, Xi'an 710100, China
[c] Key laboratory of Flexible Electronics of Zhejiang Province, Ningbo Institute of Northwestern Polytechnical University, Ningbo 315103, China
[d] MIIT Key Laboratory of Flexible Electronics, Northwestern Polytechnical University, Xi'an 710072, China

ARTICLE INFO

Article history:
Received 10 January 2024
Revised 3 February 2024
Accepted 14 March 2024
Available online 16 March 2024

Keywords:
Li metal batteries
Solid electrolyte interphase
High voltage
Fluorinated electrolyte
Electrolyte decomposition

ABSTRACT

Fluoride-based electrolyte exhibits extraordinarily high oxidative stability in high-voltage lithium metal batteries (h-LMBs) due to the inherent low highest occupied molecular orbital (HOMO) of fluorinated solvents. However, such fascinating properties do not bring long-term cyclability of h-LMBs. One of critical challenges is the interface instability in contacting with the Li metal anode, as fluorinated solvents are highly susceptible to exceptionally reductive metallic Li attributed to its low lowest unoccupied molecular orbital (LUMO), which leads to significant consumption of the fluorinated components upon cycling. Herein, attenuating reductive decomposition of fluorinated electrolytes is proposed to circumvent rapid electrolyte consumption. Specifically, the vinylene carbonate (VC) is selected to tame the reduction decomposition by preferentially forming protective layer on the Li anode. This work, experimentally and computationally, demonstrates the importance of pre-passivation of Li metal anodes at high voltage to attenuate the decomposition of fluoroethylene carbonate (FEC). It is expected to enrich the understanding of how VC attenuate the reactivity of FEC, thereby extending the cycle life of fluorinated electrolytes in high-voltage Li-metal batteries.

Building better batteries with high energy density and safety are core enthusiasm to power electric vehicles and portable electronics [1–3]. The lithium (Li) metal anode is experiencing tremendous growth of interests as an appealing alternative to the current graphite anode in energy-demanding battery chemistries due to its champion capacity (3860 mAh/g) [4–11]. However, the highly reactive Li metal anode inevitably side-reacts with the electrolyte and forms a fragile solid electrolyte interphase (SEI) [12–16], leading to uncontrolled Li dendrite propagation, constant electrolyte consumption, and violent Li interface fluctuation during repetitive lithium plating/striping [17–19].

These issues impair the Coulombic efficiency (CE) and cycle life of Li metal batteries, and plague their practical applications [20–22]. Electrolyte engineering has been proposed to circumvent the above problems by optimizing concentration, viscosity, non-flammability, and oxidative stability in specific battery systems [23–28]. So far, fluorinated electrolytes have been verified as one of the promising media for high-voltage Li metal batteries (h-LMBs) due to their excellent oxidation stability against and efficient Li striping/plating [29–33]. The anodic oxidation stability is a result of the extremely high electronegativity of fluorine atoms that withdraw electrons from entire molecular to low down the highest occupied molecular orbit (HOMO) [34,35]. The efficient Li striping/plating is attributed to the formation of a lithium fluoride (LiF) rich SEI [36]. In particular, the cyclic FEC and linear methyl(2,2,2-trifluoroethyl)carbonate (FEMC) have been probed to extend upper voltage and enable high-voltage battery cathode. The lowest unoccupied molecular orbit (LUMO) of FEC is lower than that of FEMC, indicating that FEC is prone to decompose at the Li anode to establish LiF-rich interface and that FEMC is capable of withstanding oxidation decomposition at the cathode. However, LiF-rich interface comes at the expense of violently reacting with Li metal anode. When Li^+ combines with FEC, the C—F bond tends to break down with the electron transfer proceeding. The radical anion intermediate is unstable and can be further decomposed into CO_2, resulting in a rapid FEC consumption and serious gas production at the initial stage [37,38].

* Corresponding authors.
E-mail addresses: iamzgliu@nwpu.edu.cn (Z.-G. Liu), iamybyan@nwpu.edu.cn (Y.-B. Yan), iamlkong@nwpu.edu.cn (L. Kong).

https://doi.org/10.1016/j.cclet.2024.109773
1001-8417/

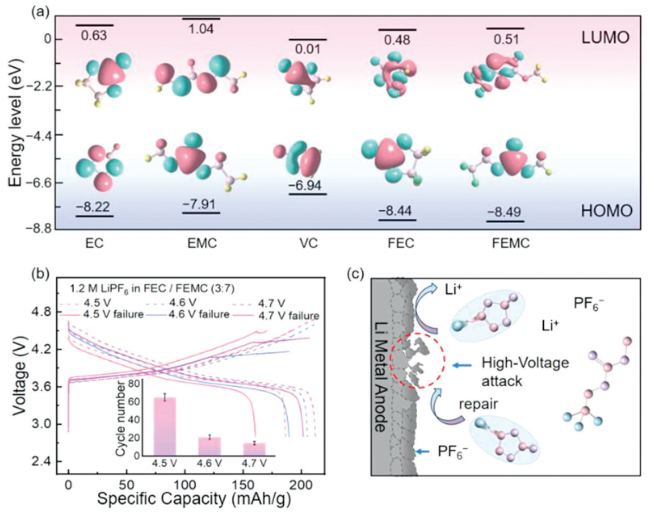

Fig. 1. (a) HOMO and LUMO energy levels of commonly used solvents. (b) Charge and discharge curves of 1.2 mol/L $LiPF_6$ in FEC/FEMC (v/v = 3:7) electrolyte under different cut-off voltages. The inset is the average cycle number of corresponding cells under different cut-off voltages. (c) Mechanistic diagram of rapid failure of 1.2 mol/L $LiPF_6$ in FEC/FEMC (v/v = 3:7) electrolyte at the high cut-off voltage.

Despite of promotion of LiF-rich SEI, extensive consumption of fluorinated solvents, like FEC, constantly varies electrolyte composition and rapidly exhausts electrolyte dosage, if Li anode is not effectively protected. Specifically, the stronger solvating capability of FEC with respect to FEMC tends to be reduced greater rapidly, resulting in less portion of charged Li-solvent complex [39–41]. This consequence corresponds to low reaction kinetics and cell death. Therefore, rational selection of fluorinated solvents and deliberate protection of reactive Li anode is of paramount importance to prolong high-volage Li metal batteries.

In this contribution, attenuating reductive decomposition of fluorinated electrolytes is achieved by applying film-forming solvents that can tame the reduction of fluorinated electrolytes through prior decomposition. The molecular orbitals of FEC and FEMC, as well as other commonly used solvents are analyzed by density functional theory (DFT) method, and compared their tendencies of reductivity on Li metal anode. To mitigate fluorinated electrolytes decomposition, VC is adopted due to following advantages: (1) The lower LUMO energy that enables prior reduction to depress FEC decomposition [42], and (2) excellent film-forming capability that promote qualified SEI to tolerate interface fluctuation [43,44]. The ternary electrolyte holds a high-voltage stability and aids an excellent SEI, due to the synergistic effects of VC and FEC. These collective benefits enable the Li||NMC622 batteries with a stable cycling performance under high voltage (4.5 V). Specifically, the life cycle of Li||NMC622 cell is extended from ~70 cycles to more than 200 cycles under a high capacity of 3.4 mAh/cm^2. Even in the higher voltage of 4.7 V, the cell attains 80% of the initial capacity after 60 cycles. This work provides a new view to attenuate reductive decomposition of fluorinated electrolytes for high-voltage Li metal batteries.

The relative reaction activity of solvents can be theoretically determined by the energy orbitals of the molecules. The higher HOMO energy implies the lower oxidative decomposition potential [45,46], while the lower LUMO energy indicates the higher reductive decomposition potential. The DFT calculations are used to probe the theoretical HOMO/LUMO energies of fluorinated carbonate-based solvents (FEC and FEMC) and conventional carbonate-based solvents (EC and EMC), as shown in Fig. 1a. The HOMO/LUMO energies of the FEC are calculated to be −8.44 eV and 0.48 eV, respectively, which are more negative than that of the EC (−8.22 eV and 0.63 eV). The fluorinated linear FEMC exhibits lower HOMO/LUMO energies (−8.49 eV and 0.51 eV) than that of EMC (−7.91 eV and 1.04 eV). These results strongly suggest that fluorinated solvents with low HOMO/LUMO levels are likely to exhibit greater oxidation resistance and easier reduction tendency than their counterparts.

Based on the above analysis, 1.2 mol/L lithium hexafluorophosphate ($LiPF_6$) is dissolved in FEC/FEMC mixture with different volume ratios, which are served as the electrolyte for the assembly of Li||NCM622 cells. The cycling performances of individual electrolyte formulation are tested at high cut-off voltages of 4.5, 4.6 and 4.7 V (Fig. S1 in Supporting information). When the FEC in the electrolytes account for 30 vol%, the average CE, cycle number and discharge capacity of the cells are maintained at 99.7%, ~70 cycles, and 4.42 mAh/cm^2, respectively. If the FEC in the electrolytes account for 50 vol%, the average CE, cycle number and discharge capacity of the cells are maintained at 99.53%, ~30 cycles, and 4.3 mAh/cm^2, respectively. It is noted that greater (50 vol%) or less (<30 vol%) FEC percentage in the electrolyte cannot deliver desired battery performances, with the average CE <95% (Figs. S1-S4 in Supporting information) and lifetime <20 cycles under high cut-off voltages (4.6 and 4.7 V). Two factors restrain the FEC content in an appropriate range in the electrolyte composition. First, extremely high FEC content promote a large amount of gases upon cycling, and high melting point of FEC increase viscosity of electrolyte, damaging the cell performances [47,48]. Second, in the case of low FEC content, mild solvation capability of the entire electrolyte cannot disassociate Li salts, and the large presence of uncharged species, such as contact ion pair (CIP) and aggregate (AGG) [49,50], adversely impact ion mobility, rate capability and cyclability [51]. Accordingly, this study takes 30 vol% FEC as an optimal composition to detailly probe their battery performances with the aid of attenuating the reductive decomposition of fluorinated electrolytes.

The cell with 30 vol% FEC in electrolyte fails after ~70 cycles at a voltage of 4.5 V, and its cycle life shortens to 20 and 10 cycles at upper voltage thresholds of 4.6 V and 4.7 V, respectively (Fig. 1b). The rapid capacity decay with increasing upper voltages is ascribed to the progressive decomposition of FEC. Firstly, FEC inherits a large dielectric constant of EC, endowing it with high electron donicity to enter inner sheath of Li [52]. It benefits the formation of solvent separated ion pair (SSIP) to carry charges for ion transport. Secondly, as shown in Fig. S5 (Supporting information), the charge distribution shows that there are more negative electric charges around the fluorine atoms in the FEC molecule, and the electronegativity of fluorine is so large that the atomic nucleus attracts the outer electrons more strongly, which results in the FEC molecule attracting electrons more easily. There are fewer negative charges around the oxygen atom in FEC compared to EC, which means that FEC is more likely to accept negative electrons and undergo reduction reactions compared to EC. Therefore, FEC is readily decomposed and continuously reduced, leading to the electrolyte composition mimic to the low FEC scenario (*e.g.*, 10 vol% FEC), which cannot deliver prolonged cycle life under high-voltage condition. FEMC is a linear carbonate with a low dielectric constant [53], which exhibit mild solvation capability to interact with Li, which therefore is excluded from the first solvated sheath of Li^+. The low HOMO energy level of FEMC further improve electrolyte stability [54].

This suggested scenario is illustrated in Fig. 1c. The FEC has a low LUMO energy level, which endows it with preferentially and continuously decomposing at Li metal anode to form a LiF-rich SEI. The fluctuation of Li surface crushes the SEI and exposes fresh Li surface. When Li metal is exposed on the anode surface, there is no dense SEI for protection, and the electrons generated by the external circuit will be transferred to the lithium metal surface. The FEC gets electrons and undergoes a reduction reaction in contact

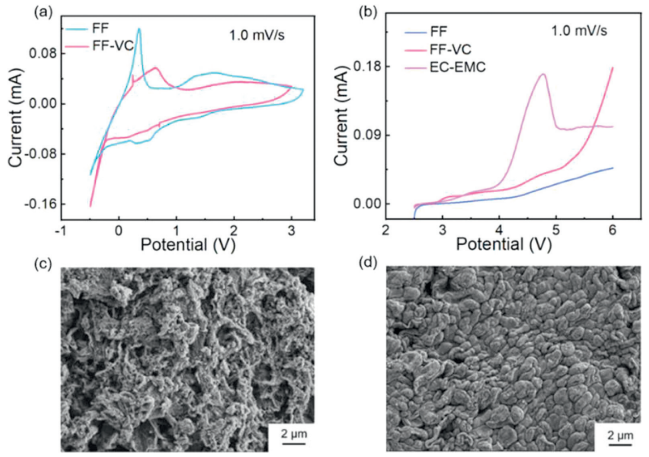

Fig. 2. (a) CV curves of Li||Cu cells with different electrolytes at a scanning rate of 1 mV/s. (b) LSV curves of Li||Al cells at a scanning rate of 1 mV/s in different electrolytes. SEM images of Li metal surface in Li||NCM622 cells with (c) FF and (d) FF-VC electrolytes after 60 cycles at the 4.5 V cut-off voltage.

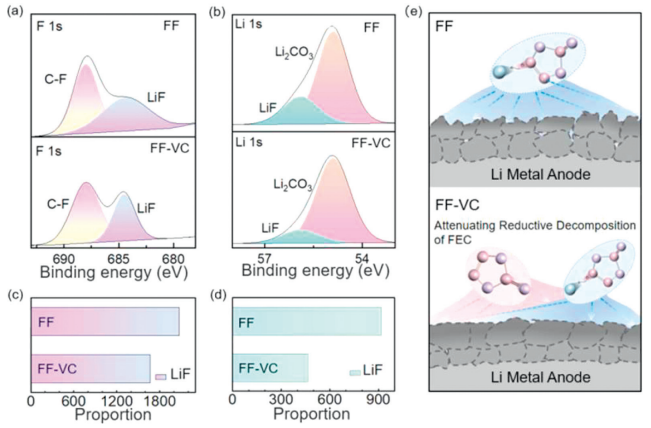

Fig. 3. Probing surface composition of the Li metal anode. (a) F 1s and (b) Li 1s XPS of the Li anodes after 20 cycles in FF and FF-VC electrolytes. The relative LiF contents in SEI derived from FF and FF-VC electrolytes, which are calculated based on (c) F and (d) Li spectra. (e) Schematic presentation of the benefits of the VC in FF electrolyte.

with the Li metal surface, which will lead to further decomposition of the FEC. Such repetitive FEC decomposition and SEI repairing progressively deplete electrolyte component and cause cell failure. To verify the above analysis, cyclic voltammetry (CV) measurements were carried out in two single-solvent electrolytes, namely 1.2 mol/L $LiPF_6$ in FEC and FEMC, respectively (Fig. S6 in Supporting information). In the FEC electrolyte, it has a higher reduction potential compared to that of the FEMC electrolyte.

Although FEC-based electrolytes can be adapted to the high cut-off voltages. However, the violent reductive decomposition of FEC on the Li metal anode consumes FEC during the cycling, resulting in insufficient cycle life. Therefore, attenuating fluorinated component reduction and optimizing the electrolyte formulation are of outmost importance for building long-lasting Li metal batteries. The C=C bond in VC molecule render it to be more readily reduced compared with FEC, since the LUMO energies of VC (0.01 eV) is lower than that of FEC (0.48 eV). As a film-forming additive [55,56], VC preferentially forms an effective SEI layer on the Li metal anode, supporting the rapid Li^+ ion plating/stripping. The VC-derived dense SEI has the possibility to attenuate FEC consumption. To better understand the sequence of electrolyte component decomposition on Li metal anode, the CV curves of Li||Cu cells were measured (Fig. 2a). The experiment results show that, during the initial cathodic process, the reductive current of the cell with the FF-VC electrolyte (1.2 mol/L $LiPF_6$ in FEC/FEMC/VC with a volume ratio of 3/6/1) is higher than the cell with the FF electrolyte (1.2 mol/L $LiFP_6$ in FEC/FEMC with a volume ratio of 3/7), indicating that VC is preferentially reduced at the Li anode. The anodic stability of electrolytes is investigated by LSV curves. As shown in Fig. 2b, the oxidation voltage of FF-VC electrolyte is still at a high level with respect to commercial electrolyte (EC/EMC), indicating that FF-VC electrolyte has the possibility to endure high-voltage Li metal batteries.

In order to investigate the attenuating decomposition of the fluorinated electrolyte, the morphologies of the Li metal anodes after cycling were characterized by scanning electron microscope (SEM). As shown in Fig. 2c, the Li metal anode with FF electrolyte shows a rough and porous structure with the Li dendrite aggregating into crosslinked interface. The severe electrolyte depletion and the dead Li formation are proved by the mossy and porous Li deposition. Such inhomogeneous Li deposition causes impedance increase, cells failure and safety risk. This issue is exaggerated by the increase of cut-off voltage. On the contrary, the presence of VC in FF electrolyte induces uniform and dense Li plating (Fig. 2d). It can be attributed to the prior decomposition of VC to form dense SEI, which attenuated further reduction of FEC. The slight FEC decomposition instead of violent FEC depletion reinforces the fluorinated SEI while prevents rapid change of electrolyte composition upon cycling.

High-resolution X-ray photoelectron spectroscopy (XPS) of Ar sputtering was utilized to analyze the component of the SEIs (Figs. 3a and b). The LiF peak for the Li metal surface with FF electrolyte is much stronger and sharper than that of FF-VC electrolyte. Quantitative analysis of LiF contents (Figs. 3c and d) in two sets of electrolyte derived interface demonstrates that the addition of VC in fluorinated electrolyte significantly attenuates reductive decomposition of FEC, inhibiting the large amount of LiF generation.

On the basis of chemical composition of Li metal surface revealed by XPS profiles, attenuating the fluorinated electrolytes with the aid of protective surface is schematically summarized in Fig. 3e. In the case where only fluorinated solvents exist in the electrolyte, FEC decomposes rapidly to form SEI in the early stage, which lead to the rapid depletion of FEC. FEC along cannot be able to maintain the subsequent stability of the SEI. When the VC is added to the FF electrolyte, the lower LUMO energy level of VC compared with FEC enables VC preferentially decomposing and thus developing protective layer to attenuate the reductive decomposition of fluorinated electrolyte. On the other hand, the VC and FEC will cooperatively interact to form a dense and dendrite-free SEI on the Li metal surface, endowing the long cycle life of Li metal batteries with high-voltage operation.

Given that the addition of the VC to the baseline fluorinated electrolytes confers the better anode stability against Li metal anode, Li||Li symmetric cells are supposed to deliver enhanced performances (Fig. S7 in Supporting information). The cell with FF-VC electrolyte has a larger polarization voltage than the cell with the FF electrolyte, which is attributed to the fact that FEC form a robust LiF-rich SEI during the initial cycling process. LiF-rich SEI can promote the diffusion of Li ions and decrease the nucleation overpotential of Li plating in symmetric cells [57]. The preferential reduction of VC results in the qualified SEI containing the polymerized VC, which contribute to the tame Li ions conductivity and slightly high nucleation overpotential (Fig. S7). Despite of low overpotential of FF based symmetric cell, the rapidly consumed FEC cannot timely repair the ruptured SEI, leading to the internal short circuit after 420 h.

Cells are then assembled by coupling the Li metal anodes with the high-areal-capacity NCM622 cathodes (5.5 mAh/cm^2) to eval-

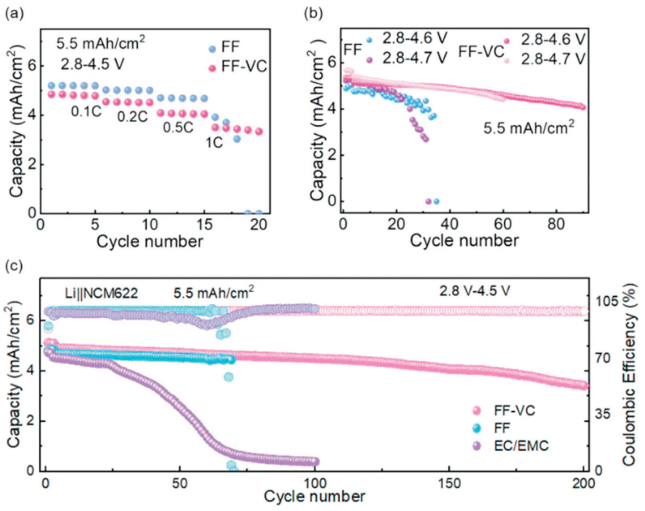

Fig. 4. Electrochemical performances of Li||NCM622 cells. (a) Rate capability of cells at the voltage of 4.5 V. (b) Cycle stability of cells with FF and FF-VC electrolytes under the cut-off voltages of 4.6 V and 4.7 V. (c) Long cycle stability of cells with different electrolytes under the cut-off voltage of 4.5 V.

uate the cell performances. As shown in Fig. 4a, the poor rate performance of the cell with pristine FF electrolyte cannot sustain high rate current due to fragile SEI, while VC-derived SEI impart sufficient robustness to withstand high-rate output (1 C), delivering the initial capacity around 190 mAh/g. The corresponding charge/discharge curves are shown in Fig. S8 (Supporting information).

In order to evaluate the high-voltage stability of the cells with different electrolytes, Li||NCM622 cells are assembled (Fig. 4b). The cell with FF electrolyte experiences a rapid capacity decay at 4.6 V and 4.7 V due to the consumption of FEC. The life spans of high-voltage cells are significantly extended in the FF-VC electrolyte, achieving 4.06 mAh/cm^2 and 4.42 mAh/cm^2 after 60 and 92 cycles, respectively.

To demonstrate the superiority of VC aided fluorinated electrolyte, the cells are cycled between 2.8–4.5 V (Fig. 4c). The corresponding charge/discharge curves are shown in Fig. S9 (Supporting information), where the batteries are cycled at a rate of 0.2 C. The capacity of the cell using conventional EC/EMC electrolyte shows a sharp fading after 20 cycles, since the de-fluorinated electrolyte cannot endure high-voltage operation. Although the cell with FF electrolyte can work well in the initial cycles, the rapid consumption of fluorinated electrolyte leads to the sudden cell death after ~70 cycles. In contrast, the protected Li anode with VC attenuates the FEC decomposition, attaining 3.4 mAh/cm^2 after 200 cycles.

In conclusion, this study proposes a strategy that involves attenuating fluorinated electrolyte decomposition by taking film-forming additive. This strategy is applicable in the broad scope that the high-voltage electrolyte suffering reductive decomposition can be tamed by priorly protecting Li metal anode. Specifically, the attenuating reductive decomposition of FEC by VC provides insights into the fundamental interactions between fluorinated electrolytes and non-fluorinated electrolytes, leading to a deeper understanding of the degradation mechanisms of fluorinated electrolytes, highlighting the importance of stabilizing anode surface when applying high anodic decomposition electrolyte. This work enables long-term high-voltage operating stability of high-energy Li||NCM622 batteries up to 4.6 V.

Declaration of competing interest

The authors declare no conflict of interest.

Acknowledgments

This work was supported by the National Natural Science Foundation of China (Nos. 22379121, 62005216), Basic Public Welfare Research Program of Zhejiang (No. LQ22F050013), Zhejiang Province Key Laboratory of Flexible Electronics Open Fund (2023FE005), and Shenzhen Foundation Research Program (No. JCYJ20220530112812028). We thank Ms. Fang-Fang Wang, Mr. Xiong Xiao and Ms. Jia-Yue Duan for helpful discussion.

Supplementary materials

Supplementary material associated with this article can be found, in the online version, at doi:10.1016/j.cclet.2024.109773.

References

[1] S. Ling, B. Deng, R. Zhao, et al., Adv. Energy Mater. 13 (2023) 2202847.
[2] C. Yang, Appl. Energy 306 (2022) 118116.
[3] C. Yang, H.J. Shi, Int. J. Low Carbon Technol. 18 (2023) 1134–1139.
[4] P. Shi, X.Q. Zhang, X. Shen, et al., Adv. Mater. Technol. 5 (2020) 1900806.
[5] S. Zhang, B. Cheng, Y. Fang, et al., Chin. Chem. Lett. 33 (2022) 3951–3954.
[6] L. Chen, X. Fan, X. Ji, et al., Joule 3 (2019) 732–744.
[7] H. Wu, Y. Xu, X. Ren, et al., Adv. Energy Mater. 9 (2019) 1902108.
[8] Y. Xu, Y. Zhou, T. Li, et al., Energy Storage Mater. 25 (2020) 334–341.
[9] C.B. Jin, N. Yao, Y. Xiao, et al., Adv. Mater. 35 (2023) 2208340.
[10] L. Ding, X. Yue, X. Zhang, et al., Proc. Natl. Acad. Sci. U. S. A. 120 (2023) e2314264120.
[11] C.Z. Zhao, Q. Zhao, X. Liu, et al., Adv. Mater. 32 (2020) 1905629.
[12] Q.K. Zhang, X.Q. Zhang, J. Wan, et al., Nat. Energy 8 (2023) 725–735.
[13] B. Zhao, L. Ma, K. Wu, et al., Chin. Chem. Lett. 32 (2021) 125–131.
[14] M. Zhang, R. Liu, Z. Wang, et al., Chin. Chem. Lett. 31 (2020) 1217–1220.
[15] Z. Li, N. Fu, Z. Yang, Particuology 83 (2023) 129–141.
[16] J.Y. Duan, J.X. Chen, F.F. Wang, et al., J. Energy Chem. 87 (2023) 473–478.
[17] L. He, Q. Sun, L. Lu, et al., ACS Appl. Mater. Interfaces 13 (2021) 34320–34331.
[18] M. Ge, X. Zhou, Y. Qin, et al., Chin. Chem. Lett. 33 (2022) 3894–3898.
[19] P. Hundekar, R. Jain, A.S. Lakhnot, et al., J. Appl. Phys. 128 (2020) 010903.
[20] L. Su, A. Manthiram, Small Struct. 3 (2022) 2200114.
[21] Q. Dong, M. Wang, X. Huang, et al., ACS Appl. Mater. Interfaces 15 (2023) 17386–17395.
[22] X.Z. Fan, M. Liu, R. Zhang, et al., Chin. Chem. Lett. 33 (2022) 4421–4427.
[23] C. Li, Y. Li, Z. Chen, et al., Chin. Chem. Lett. 34 (2023) 107852.
[24] M. Xia, M. Lin, G. Liu, et al., Chem. Eng. J. 442 (2022) 136351.
[25] Z. Chu, S. Zhuang, J. Lu, et al., Chin. Chem. Lett. 34 (2023) 107563.
[26] B. Jiang, H. Li, B. Luo, et al., Chin. Chem. Lett. 35 (2024) 108649.
[27] L. Shen, C. Xu, J. Gao, et al., J. Energy Chem. 77 (2023) 348–358.
[28] W. Yu, N. Deng, L. Tang, et al., Particuology 65 (2022) 51–71.
[29] J. Xie, S.Y. Sun, X. Chen, et al., Angew. Chem. Int. Ed. 61 (2022) e202204776.
[30] Y. Huang, Y. Zhu, H. Cheng, et al., Chin. Chem. Lett. 34 (2023) 107711.
[31] W. Cai, Y. Deng, Z. Deng, et al., Adv. Energy Mater. 13 (2023) 2301396.
[32] G.B. Berhe, W.N. Su, T.T. Hagos, et al., J. Power Sources 558 (2023) 232567.
[33] C. Zhang, Nat. Energy 4 (2019) 350.
[34] P. Xiao, Y. Zhao, Z. Piao, et al., Energy Environ. Sci. 15 (2022) 2435–2444.
[35] N. von Aspern, G.V. Röschenthaler, M. Winter, et al., Angew. Chem. Int. Ed. 58 (2019) 15978–16000.
[36] Y.H. Tan, G.X. Lu, J.H. Zheng, et al., Adv. Mater. 33 (2021) 2102134.
[37] H. Moon, H. Nam, M.P. Kim, et al., Adv. Funct. Mater. 33 (2023) 2303029.
[38] L. Zhang, F. Min, Y. Luo, et al., Nano Energy 96 (2022) 107122.
[39] C.C. Su, M. He, M. Cai, et al., Nano Energy 92 (2022) 106720.
[40] X. Hu, J. Liu, Y. Yang, et al., Chin. Chem. Lett. 34 (2023) 108456.
[41] M. Fang, B. Du, X. Zhang, et al., Angew. Chem. Int. Ed. 63 (2024) e202316839.
[42] M. Fang, X. Yue, Y. Dong, et al., Joule 8 (2024) 91–103.
[43] P.G. Kitz, M.J. Lacey, P. Novák, et al., J. Power Sources 477 (2020) 228567.
[44] Y. Jin, N.J.H. Kneusels, L.E. Marbella, et al., J. Am. Chem. Soc. 140 (2018) 9854–9867.
[45] W. Zhang, S. Zhang, L. Fan, et al., ACS Energy Lett. 4 (2019) 644–650.
[46] Q. Liu, W. Jiang, J. Xu, et al., Nat. Commun. 14 (2023) 3678.
[47] X. Zheng, G. Fang, Y. Pan, et al., J. Power Sources 439 (2019) 227081.
[48] D. Aurbach, E. Markevich, G. Salitra, J. Am. Chem. Soc. 143 (2021) 21161–21176.
[49] J. Zhang, Q. Fu, P. Li, et al., Particuology 89 (2024) 238–245.
[50] C. Tian, K. Qin, L. Suo, Mater. Futures 2 (2023) 012101.
[51] S. Duangdangchote, N. Phattharasupakun, P. Chomkhuntod, et al., Chem. Commun. 57 (2021) 6732–6735.
[52] Z. Wang, Z. Sun, Y. Shi, et al., Adv. Energy Mater. 11 (2021) 2100935.
[53] C.C. Su, M. He, R. Amine, et al., Energy Environ. Sci. 12 (2019) 1249–1254.
[54] T. Cao, S. Huang, Y. Sun, et al., J. Phys. Chem. C 126 (2022) 5122–5130.
[55] P. Jankowski, W. Wieczorek, P. Johansson, J. Mol. Model. 23 (2016) 6.
[56] G. Zheng, Y. Xiang, S. Chen, et al., Energy Storage Mater. 29 (2020) 377–385.
[57] B.R. Das Goswami, V. Jabbari, R. Shahbazian-Yassar, et al., J. Phys. Chem. C 127 (2023) 21971–21979.